Superior strength and wear resistance of mechanically deformed High-Mn TWIP steel

Olugbade, Temitope Olumide; Oladapo, Bankole I.; Ting, Tin Tin

Published in:
Colloids and Surfaces A: Physicochemical and Engineering Aspects

DOI:
10.1016/j.colsurfa.2024.134388

Publication date:
2024

Colloids and Surfaces A: Physicochemical and Engineering Aspects 696 (2024) 134388

Contents lists available at ScienceDirect

Colloids and Surfaces A: Physicochemical and Engineering Aspects

journal homepage: www.elsevier.com/locate/colsurfa

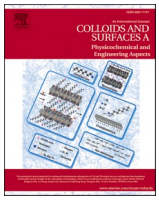

Superior strength and wear resistance of mechanically deformed High-Mn TWIP steel

Temitope Olumide Olugbade [a,b,*], Bankole I. Oladapo [a,b], Tin Tin Ting [b]

[a] School of Science and Engineering, University of Dundee, Dundee, UK
[b] Faculty of Data Science and Information Technology, INTI International University, Persiaran Perdana BBN, Putra Nilai, Malaysia

GRAPHICAL ABSTRACT

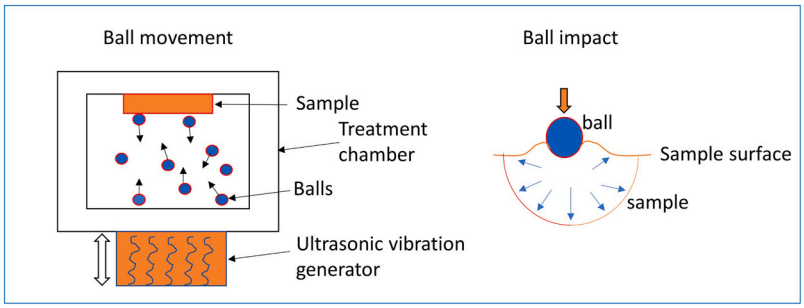

ARTICLE INFO

Keywords:
TWIP steel
Deformation
Microhardness
Wear
Sustainable manufacturing

ABSTRACT

In the present study, the mechanical and wear behaviour of the surface-mechanically treated high-manganese (high-Mn) twinning-induced plasticity (TWIP) steel were investigated. The TWIP alloy was first designed and fabricated via surface-mechanical attrition treatment (SMAT) system and the mechanical properties including strength, wear behaviour as well as the microstructural evolution were thereafter determined. Transmission electron microscopy (TEM) characterization revealed a typical dislocation as a result of the surface treatment as well as the formation of twin layers with a reduced stacking fault energy (SFE). Due to the ultra-fine grain refinement caused by plastic deformation during surface treatment, a microhardness value of 489 HV can be obtained after treatment. Likewise, the yield strength of the high-Mn TWIP steel could be enhanced from 360 MPa to 813 MPa and a reduction in elongation to failure of about 20 % can be achieved. The wear test showed that the treated TWIP steel possessed a reduced friction coefficient and improved wear resistance at different testing loads, attributed to the nanoscale refinement of grains induced during treatment. The strength, hardness, and wear resistance of the fabricated TWIP alloy improves significantly, thanks to surface treatment by SMAT.

* Corresponding author at: School of Science and Engineering, University of Dundee, Dundee, UK.
E-mail address: tolugbade001@dundee.ac.uk (T.O. Olugbade).

https://doi.org/10.1016/j.colsurfa.2024.134388
Received 21 April 2024; Received in revised form 21 May 2024; Accepted 26 May 2024
Available online 27 May 2024

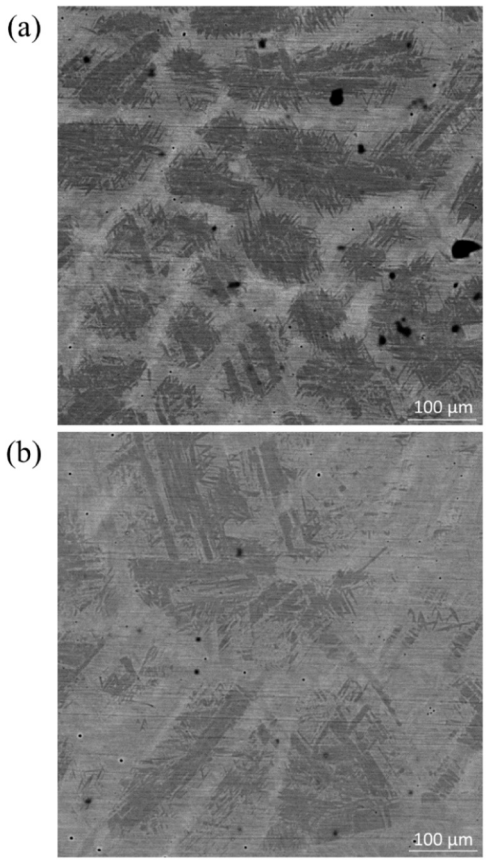

Fig. 1. Surface microstructures of the fabricated high-Mn TWIP steels revealing the formation of twins on sample surface, (a) as-received, and (b) treated.

1. Introduction

Twinning-induced plasticity (TWIP) alloys are widely recognized and considered material of choice for many automobile industries due to the remarkable properties it possesses such as improved strain hardening, high strength, and excellent ductility [1–3]. Mostly, aerospace companies prefer the use of TWIP alloys due to their high energy absorption property when compared to many other traditional high-strength steels [2]. TWIP effect and alloying (with Mn as the primary element) are the major factors responsible for the enhanced properties in TWIP alloys, unlike the traditional Cr-Ni steels where Ni is the primary alloying element [3]. TWIP steels typically contain Fe-Mn-C-Al-Si with the percentage of Mn more than 25 % [1]. It is important to know that Mn-alloying in TWIP steels maintains the stacking fault energy (SFE) as well as the austenitic structure at room temperature.

During deformation process, materials with deformation induced twinning such as TWIP steels possesses outstanding plasticity, and this remarkable behaviour could be attributed to several factors including the shortened twin boundary along the dislocation route, prompt paths for dislocation movement from the twin boundaries, and the beneficial orientations of twin-slip deformation [4–6]. For instance, the high-strain hardening rate was obtained for the laser powder fabricated-$Fe_{47}Mn_{30}Co_{10}Cr_{10}Ni_3$ alloy [4] under high strain leading to outstanding plasticity even at low temperatures. This may be accrued to the rapid formation of deformation twinning at moderate speed thereby avoiding strain localization in the process. This mechanism applies to other alloys such as high SFE $FeMn_{17.5}Al_{8.3}C_{0.74}Si_{0.14}$ alloy [7] due to substructure-induced twinning, $FeMn_{22}Al_3Si_3$ alloy [8] with enhanced work-hardening, $FeCu_xMn_{3.0}Ni_{1.5}Al_{1.5}$ alloy [9], supra-ductile $FeMn_{15}Al_2Si_2$ TWIP steel deforming at high strain rates [10], and other polycrystalline alloys [11–13]. To this end, it is necessary to understand the relationship between strain hardening behaviour, deformation mechanism, and SFE for designing high-Mn TWIP steels.

However, high-Mn TWIP steel still experiences failure when loaded or in use which often initiates at the material surface and propagates to the matrix until a final rupture occurs. Hence, the need for surface modification process to enhance the material properties is necessary. Several techniques have been applied to enhance the overall properties of materials among which are shot peening, electrodeposition and coatings [14–17], ultrasonic peening, cold working, and SMAT [18–22]. Among the surface treatment methods, SMAT is considered as a good method of improving the materials properties with less effects on their

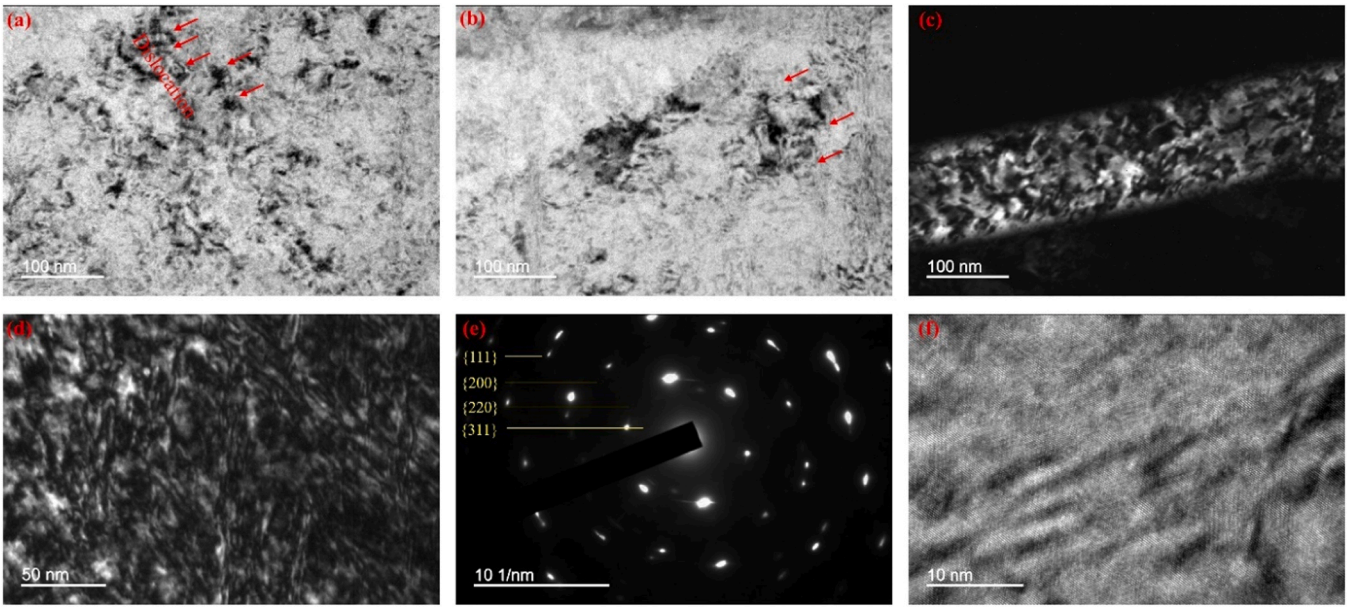

Fig. 2. TEM micrographs of the high-Mn TWIP steel; (a) typical dislocation caused by surface treatment, (b) bright-field micrograph, (c) and (d) dark-field micrographs, revealing the twin layers, (e) corresponding selected area electron diffraction (SAED) patterns of (d), (f) HRTEM image revealing the twin layers and stacking fault.

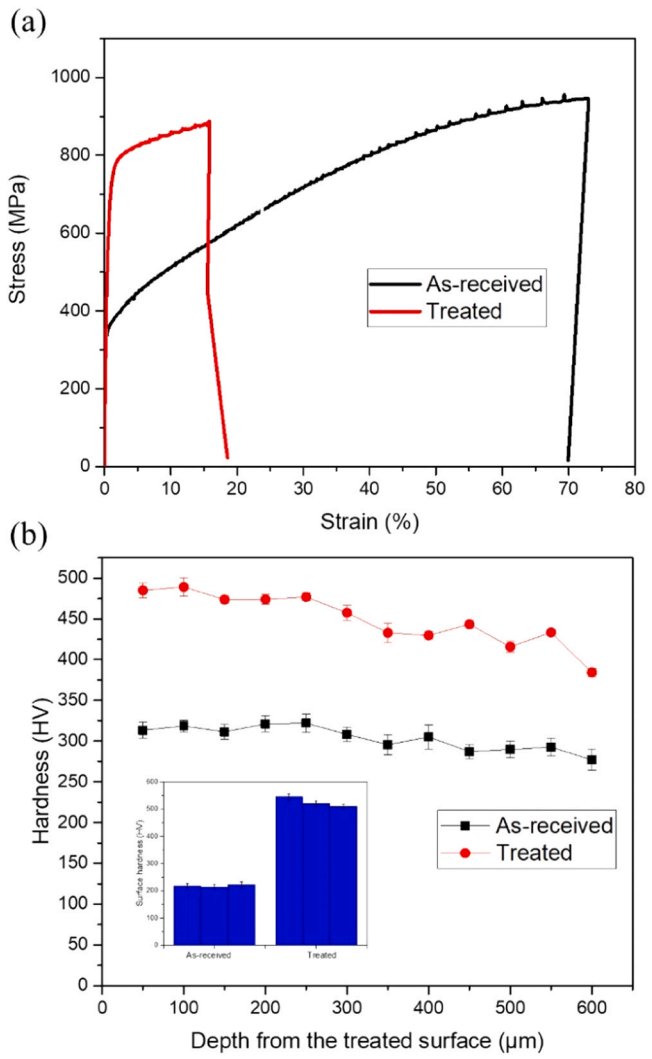

Fig. 3. Mechanical properties of the as-received and treated high-Mn TWIP steels, (a) tensile engineering stress–strain curve, (b) the microhardness distribution across the depth from the treated surface. The insert represents the surface microhardness of the samples with 300 mN load and dwell time of 20 s.

original compositions [23–26]. This is done by the generation of structured layers on the material surface due to plastic deformation caused from the collision of the sample surface by high-velocity moving shots. The SMAT system has been successfully applied on various metallic materials such as Fe, Ti, Cu, stainless steels, and alloys in the past [26–32].

To the best of our knowledge, the mechanical strengthening and wear performance of high-Mn TWIP steel processed by SMAT technique has not been fully investigated. Hence, the present paper unravels the strengthening mechanism in the surface-mechanically treated TWIP steel. The microstructures before and after SMAT treatment, as well as the wear tests were obtained and analyzed. The friction coefficient before and after treatment under different loads was recorded and analyzed.

2. Experimental

2.1. Materials and preparation

A commercial high-Mn TWIP steel (1.8 mm thick) received from a vendor with chemical composition by wt% (Fe-Mn_{18}-$C_{0.75}$-$Al_{1.7}$-$Si_{0.5}$) was used in the present study. The as-received sample in hot-rolled sheets form was later subjected to surface treatment by SMAT on both sides (for equal treatment) for 5 mins using 2 mm tungsten carbide (WC) balls (mass is 20 g), and 20 Hz vibrating frequency. The random free-moving balls repeatedly hit the sample surface, thereby causing a plastic deformation. The chamber diameter is 70 mm while the length of fly of balls is kept constant at 35 mm. The SMAT set-up has been previously explained in literature [18,20,31]. The surface topography of the TWIP alloys were obtained by 20 kV FEI-Quanta 450 FEG-SEM. The TEM samples were prepared by focused-ion beam (Germany) technique and the TEM observations were carried out on JEOL-2100 F (FE-TEM, 200 kV).

2.2. Mechanical and tribology tests

The tensile tests were performed using a dog-bone sample on the "MTS, USA" Alliance RT 30 kN electro-mechanical testing equipment (extensometer - MTS 632.24 F-50) with the tensile speed of 1.5 mm/min. The UTS, YS, and fracture elongation data were collected from the stress-strain curve. A variation in microhardness along different layers after treatment was investigated via Vickers micro-hardness testing equipment (Fischer HM2000XY) with dwell time of 20 s and 300 mN load to investigate the effect of surface modifications on the hardness of the TWIP steels. Under different loads of 2, 5, 7, and 10 N, the dry-sliding wear tests were carried out in bi-wear mode by a wear testing machine (TEER ST-3001) using WC balls (Ø4 mm) with a 15 min sliding duration, 3 mm stroke length, and 1.5 mm/min sliding velocity. The profiles of the wear tracks for the TWIP samples were thereafter analyzed using surface profilometer (Veeco-Wyko NT9300). Based on the wear tracks, the wear volume obtained was analyzed by the software on the profilometer.

3. Results

3.1. Microstructures

The surface microstructures (in backscattered electrons – BSE mode) of the bare and treated TWIP steel sample are illustrated in Fig. 1. The bare TWIP steel (Fig. 1a) shows an initial grain size of about 15 – 20 μm which is evenly presented on the entire sample surface, and the formation of twins depicting the austenitic nature and a characteristic feature of a typical TWIP steel. Compared with the bare sample with the visible grain size, there is a decrease in grain size for the treated sample (Fig. 1b) which is ascribed to the plastic deformation and grain refinement due to the effect of internal compressive residual stress induced during the treatment. However, there still exists the presence of twins on the larger region of the sample.

Fig. 2 presents the TEM micrographs of high-Mn TWIP steel. A typical dislocation induced by SMAT, and the corresponding bright-field micrograph are revealed in Fig. (3a-b). As a result of surface treatment leading to mechanical deformations on the surface of TWIP steel samples, there exist some dislocations and surface defects with different sizes which covers over two-quarter of the surface layers, as indicated in red in Fig. 2(a) and (b). The dislocations signifying dominant deformation mode probably cause twinning and stress concentration. The mechanical twinning and dislocation storage could be considered as the main factors in explaining the mechanism behind the strain hardening in TWIP steel. Fig. 2(c) and Fig. 2(d) show the dark-field micrographs, revealing the twin layers, and the corresponding selected area electron diffraction patterns of (d) with [111], [200], [220], and [311] region axes are indicated in Fig. 2(e) with a higher mag/resolution micrograph of the fabricated TWIP steel alloys in Fig. 2(f).

3.2. Mechanical and tribological properties

The tensile engineering stress–strain curve for the bare Fe-Mn_{18}-$C_{0.75}$-$Al_{1.7}$-$Si_{0.5}$ TWIP alloy and the one subjected to SMAT treatment is

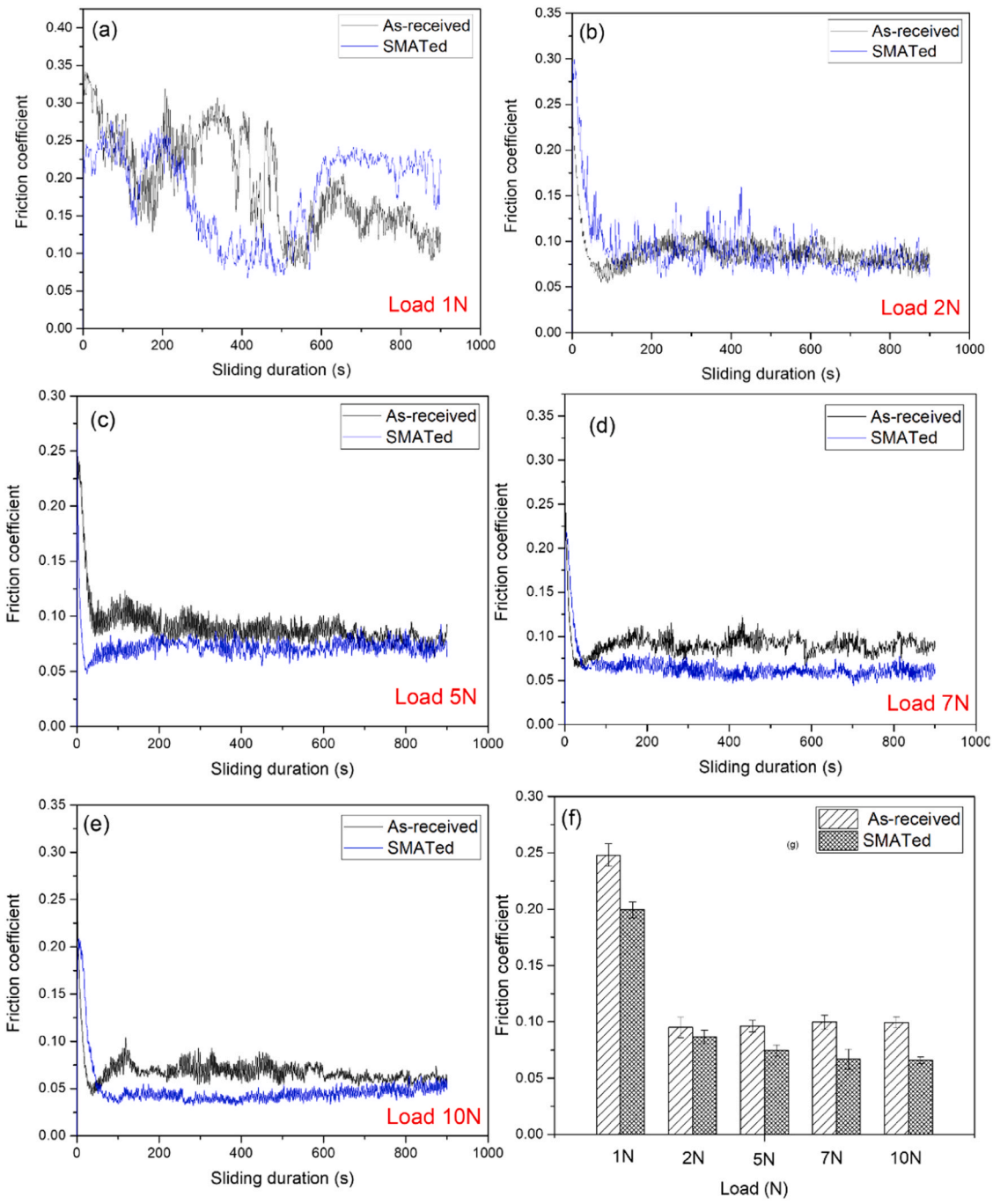

Fig. 4. Friction coefficient evolution during the wear test of as-received and treated high-Mn TWIP steels under different loads of (a) 1 N, (b) 2 N, (c) 5 N, (d) 7 N, and (e) 10 N; (f) corresponding average friction coefficient between the samples, with the applied loads.

illustrated in Fig. 3(a). The SMATed sample possessed an increased yield strength (YS) of about 813 MPa when treated for 10 mins, unlike the bare sample with the YS of ~ 360 MPa. In addition, a reduction in elongation to failure of ~20 % can be obtained after treatment compared with the untreated sample with the elongation to failure of ~ 70 %.

As revealed in Fig. 3(b), a microhardness value of 489 HV can be obtained after SMAT treatment as compared to 318 HV obtained for the untreated sample. The insert presents the surface microhardness of the TWIP steels. The microhardness after SMAT could reach as high as 544 HV compared to the untreated sample with surface hardness value of 217 HV. The improvement in the surface microhardness as well as the hardness variations across the depths can be accrued to the grain refinement process because of the plastic deformation induced during the treatment. Compressively residual stress as well as micro-strain energy induced during the treatment could also be responsible for the high hardness obtained for the treated TWIP steel sample. As a function of sliding time, the coefficient of friction evolution during the wear test under different loads are represented in Fig. 4(a-e). The corresponding average friction coefficient as a function of load between the TWIP steel samples is shown in Fig. 4(f). Compared to the bare TWIP sample, at the sliding duration of 400 s, the SMATed sample possessed a reduced friction coefficient and improved wear property at all testing loads apart from 2 N load due to the grain refinement process.

Fig. 5 shows the SEM micrographs of the worn surface of TWIP steel samples. As indicated in Fig. 5(a) which is enlarged in Fig. 5(b), there are

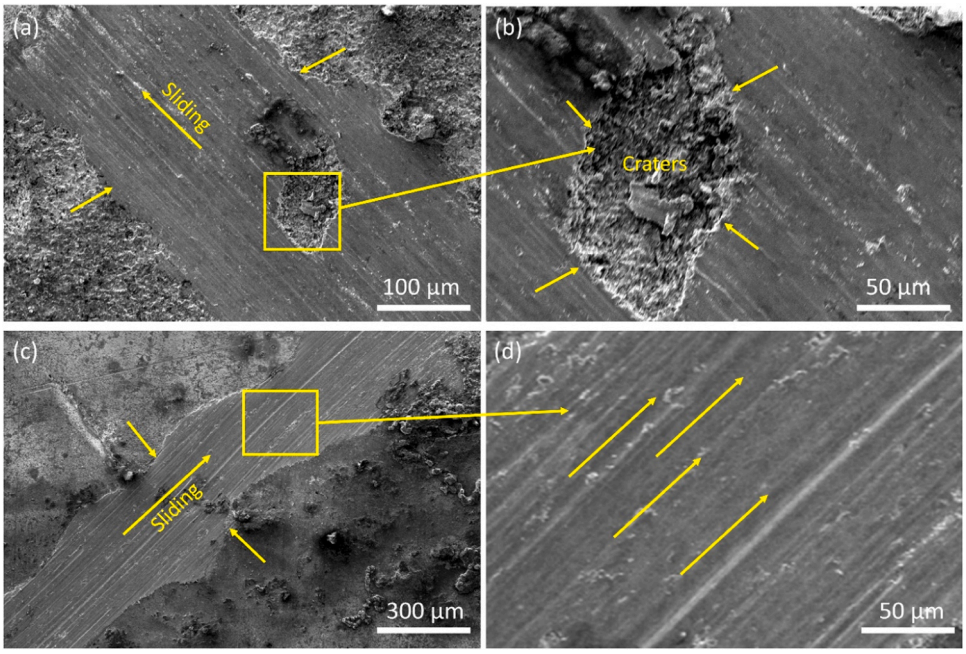

Fig. 5. Surface topography of the worn surface of high-Mn TWIP steels after wear test, (a) as-received sample, the opposite arrows indicate the wear track, (b) enlarged topography, denoted by the square box in (a), with the presence of craters, as a result of wear, (c) treated sample, the opposite arrows indicate the wear track, (d) enlarged topography, denoted by the square box in (c).

presence of craters in the untreated TWIP steel sample, because of the wear action, meanwhile the treated sample experienced less wear, as indicated in Fig. 5(c) which is enlarged in Fig. 5(d), hence an enhanced wear resistance property. This further confirms that SMAT process can enhance the mechanical properties of metallic materials.

4. Discussion

The plastic deformation and surface grain refinement caused by SMAT raised the dislocation density and suppressed the formation of mechanical twinning, as indicated in the TEM images (Fig. 2). The increase in dislocation density and suppression of mechanical twinning by plastic deformation can be attributed to the quick accumulation of dislocations by surface grain refinement in the treated high-Mn TWIP steel. This is as a result of the repeated bombardment of the sample surface with high ball velocities. A similar increase in back stress and suppression of mechanical twinning was reported by Kang et al. [33], which is attributed mainly to the plastic deformation and grain refinement effect in the TWIP steel. It is well known that a significant increase in back stress reduces the SFEs width and consequently narrows the interactions between partial dislocations required for mechanical twinning [34,35]. During the plastic deformation, a suppression in the interaction between dislocations required for twinning of Fe-3Mn-3Al-3Si TWIP sample occurred, which was attributed to the change in dislocation slip modes [35]. The cause of suppression of mechanical twinning as influenced by grain refinement can be linked to the following two reasons: (1) back stress which is caused by the accumulation of dislocations, and (2) grain boundary segregation of C atom [33,36]. During plastic deformation, it is believed that C atom can rapidly segregate and raise the SFE of the area near the grain boundaries, which can subsequently increase the dislocation formation, hence liable to suppress the mechanical twinning [37–41].

SMAT process leads to an improvement in the wear resistance and mechanical behaviour of the fabricated TWIP alloy. This can be accrued to high residual stress and grain refinement [19,21,22] induced during the treatment because of the plastic deformation resulting from the sample-balls collisions. As indicated from the friction coefficient evolution and micrographs of the worn surface, SMAT results in a reduced friction coefficients and improved wear resistance at applied loads from 1 N to 10 N. Under the different testing loads, results show that surface grain refinement caused by SMAT process lowers the coefficient of friction, hence an improved wear resistance. Several factors are thought to contribute to the variation in the coefficient of friction including lubricant influence, contact state, and contact area [42,43]. Grain refinement by SMAT induces high hardness and results in a lower contact area which subsequently leads to a reduced friction coefficient. It is believed that the smaller the contact area, the lower the coefficient of friction the better the wear resistance of metallic materials [43–45]. This is majorly due to the refinement of grains or strengthening effect of γ phase formed during the SMAT treatment [46–49].

In the present study, as evident in the micrographs of the worn surfaces (Fig. 5), many craters and debris are noticed on the untreated sample along the sliding path. Meanwhile, the case is different with the SMAT sample though some particles are present on the surface. These particles constituent the main wear mechanism. The fragments produced along the wear track can transform and oxidize into abrasive particles [50]. To sum it up, materials delamination is the primary wear mechanism for the untreated high-Mn TWIP steel whereas abrasive particles are noticed to be the primary wear mechanism for the treated sample. The abrasive particles noticed on the treated TWIP steel can be accrued to the hardness and strength caused by the grain refinement.

5. Conclusion

A high-Mn TWIP alloy was designed and fabricated via surface mechanical treatment to study the influence of the unique treatment method on surface properties and microstructures. Microstructure characterization through TEM revealed a typical dislocation induced by SMAT, as well as the formation of twin layers with a reduced SFE. Due to the ultra-fine grain-refinement via plastic deformation during SMAT, the yield strength of the high-manganese TWIP steel could be increased from 360 MPa to 813 MPa and a reduction in elongation to failure of about 20 % can be achieved. By SMAT, a microhardness value of 489 HV can be obtained after SMAT treatment as compared to 318 HV obtained for the untreated sample. SMAT process caused a significant enhancement in the surface hardness as well as the hardness variations across the

depths. The wear test showed that the treated TWIP alloys possessed reduced friction coefficients and improved wear resistance. The wear resistance and mechanical behaviour of the TWIP alloy improves significantly, thanks to surface treatment by SMAT. The high-compressive residual stress as well as the grain-refinement process are the mechanisms behind the improvement in properties and the micro-structural changes exhibited by the high-manganese TWIP alloy.

CRediT authorship contribution statement

Temitope Olumide Olugbade: Writing – review & editing, Writing – original draft, Validation, Resources, Methodology, Investigation, Conceptualization. **Bankole I. Oladapo:** Writing – review & editing, Validation, Data curation. **Tin Tin Ting:** Writing – review & editing, Resources, Funding acquisition.

Declaration of Competing Interest

The authors declare that they have no known competing financial interests or personal relationships that could have appeared to influence the work reported in this paper.

Data availability

Data will be made available on request.

Acknowledgements

Special thanks to Prof J. Lu for the SMAT technique. The effort of Dr. B. Yan for his assistance in the TEM experiment and discussion is highly acknowledged.

References

[1] O. Grassel, L. Krüger, G. Frommeyer, L.W. Meyer, High strength Fe±Mn± (Al, Si) TRIP/TWIP steels development – properties – application, Int. J. Plast. 16 (2000) 1391.
[2] Y.-K. Lee, C. Choi, Driving force for γ→ε martensitic transformation and stacking fault energy of γ in Fe-Mn binary system, Metall. Mater. Trans. A 31 (2000) 355.
[3] M.B. Kannan, R.K. Singh Raman, S. Khoddam, S. Liyanaarachchi, Corrosion behavior of twinning-induced plasticity (TWIP) steel, Mater. Corros. 64 (2013) 3.
[4] J.X. Fang, J.X. Wang, Y.J. Wang, H.T. He, D.B. Zhang, Y. Cao, Microstructure evolution and deformation behavior during stretching of a compositionally inhomogeneous TWIP-TRIP cantor-like alloy by laser powder deposition, Mater. Sci. Eng.: A 847 (2022) (2022) 143319, https://doi.org/10.1016/j.msea.2022.143319.
[5] Y. Wu, B. Deng, X. Li, Q. Li, T. Ye, S. Xiang, A. Atrens, In-situ EBSD study on twinning activity caused by deep cryogenic treatment (DCT) for an as-cast AZ31 Mg alloy, J. Mater. Res. Technol. 30 (2024) (2024) 3840–3850, https://doi.org/10.1016/j.jmrt.2024.04.099.
[6] B. Xie, H. Li, Y. Ning, M. Fu, Discontinuous dynamic recrystallization and nucleation mechanisms associated with 2-, 3- and 4-grain junctions of polycrystalline nickel-based superalloys, Mater. Des. 231 (2023) 112041, https://doi.org/10.1016/j.matdes.2023.112041.
[7] H.R. Abedi, A.Z. Hanzaki, N. Haghdadi, P.D. Hodgson, Substructure induced twinning in low density steel, Scr. Mater. 128 (2017) 69–73.
[8] D.T. Pierce, J.A. Jiménez, J. Bentley, D. Raabe, J.E. Wittig, The influence of stacking fault energy on the microstructural and strain-hardening evolution of Fe-Mn-Al-Si steels during tensile deformation, Acta Mater. 100 (2015) 178–190.
[9] Y. Zhao, Y. Sun, H. Hou, Core-shell structure nanoprecipitates in Fe-xCu-3.0Mn-1.5Ni-1.5Al alloys: a phase field study, Prog. Nat. Sci.: Mater. Int. 32 (2022) 358–368, https://doi.org/10.1016/j.pnsc.2022.04.001.
[10] G. Frommeyer, U. Brüx, P. Neumann, Supra-ductile and high-strength manganese-TRIP/TWIP steels for high energy absorption purposes, ISIJ Int 43 (2003) 438–446.
[11] Y. Zhao, K. Liu, H. Zhang, X. Tian, Q. Jiang, V. Murugadoss, H. Hou, Dislocation motion in plastic deformation of nano polycrystalline metal materials: a phase field crystal method study, Adv. Compos. Hybrid. Mater. 5 (2022) 2546–2556, https://doi.org/10.1007/s42114-022-00522-2.
[12] X. Long, K. Chong, Y. Su, C. Chang, C.L. Zhao, Meso-scale low-cycle fatigue damage of polycrystalline nickel-based alloy by crystal plasticity finite element method, Int. J. Fatigue 175 (2023) 107778, https://doi.org/10.1016/j.ijfatigue.2023.107778.
[13] X. Tian, Y. Zhao, T. Gu, Y. Guo, F. Xu, H. Hou, Cooperative effect of strength and ductility processed by thermomechanical treatment for Cu–Al–Ni alloy, Mater. Sci. Eng.: A 849 (2022) 143485, https://doi.org/10.1016/j.msea.2022.143485.
[14] B. Meng, J. Wang, M. Chen, S. Zhu, F. Wang, F, Study on the oxidation behavior of a novel thermal barrier coatoling system using the nanocrystalline coating as bonding coating on the single-crystal superalloy, Corros. Sci. 225 (2023)) (2023) 111591, https://doi.org/10.1016/j.corsci.2023.111591.
[15] T.O. Olugbade, Influence of multilayered polymer coatings on the corrosion behaviour and microstructures of Al6061-T6 alloy, Colloids Surf. A: Physicochem. Eng. Asp. 692 (2024) 133901.
[16] T. Mohammed, T.O. Olugbade, I. Nwankwo, Determination of the effect of oil exploration on galvanized steel in Niger Delta, Niger. J. Sci. Res Rep. 10 (2016) 1–9.
[17] L. Shao, N. Xue, W. Li, S. Liu, Z. Tu, Z, Y. Chen, L. Zhu, Effect of cold-spray parameters on surface roughness, thickness and adhesion of copper-based composite coating on aluminum alloy 6061 T6 substrate, Processes 11 (2023) 959, https://doi.org/10.3390/pr11030959.
[18] T.O. Olugbade, B.I. Oladapo, Q. Zhao, T.T. Tang, Strengthening and precipitation hardening mechanisms of surface-mechanically treated 17-4PH stainless steel, Int J. Adv. Manuf. Technol. (2024), https://doi.org/10.1007/s00170-024-13708-3.
[19] H. Guo, M. Xia, Z. Wu, L. Chan, Y. Dai, K. Wang, Q. Yan, M. He, C. Ge, J. Lu, Nanocrystalline-grained tungsten prepared by surface mechanical attrition treatment: microstructure and mechanical properties, J. Nucl. Mater. 480 (2017) 281–288.
[20] T.O. Olugbade, Review: corrosion resistance performance of severely plastic deformed aluminium based alloys via different processing routes, Met Mater. Int 29 (2023) 2415–2443.
[21] H. Kou, J. Lu, Y. Li, High-strength and high-ductility nanostructured and amorphous metallic materials, Adv. Mater. 26 (2014) 5518.
[22] H. Guo, M. Xia, L. Chan, K. Wang, X. Zhang, Q. Yan, M. He, J. Lu, C. Ge, Nanostructured laminar tungsten alloy with improved ductility by surface mechanical attrition treatment, Sci. Rep. 7 (2017) 1351.
[23] K. Lu, J. Lu, Nanostructured surface layer on metallic materials induced by surface mechanical attrition treatment, Mater. Sci. Eng. A 375–377 (2004) 38–45.
[24] B.N. Mordyuk, G.I. Prokopenko, M.A. Vasylyev, M.O. Iefimov, Effect of structure evolution induced by ultrasonic peening on the corrosion behavior of AISI-321 stainless steel, Mater. Sci. Eng. A458 (2007) 253–261.
[25] H.S. Lee, D.S. Kim, J.S. Jung, Y.S. Pyoun, K. Shin, Influence of peening on the corrosion properties of AISI 304 stainless steel, Corros. Sci. 51 (2009) 2826–2830.
[26] C.C. Koch, Top-down synthesis of nanostructured materials: Mechanical and thermal processing methods, Rev. Adv. Mater. Sci. 5 (2003) 91–99.
[27] T.O. Olugbade, Passivation behaviour of surface-treated 17-4PH stainless steel in chloride-containing environment with varying concentrations, Chem. Afr. 5 (2022) 333–340.
[28] T. Wang, J. Yu, B. Dong, Surface nanocrystallization induced by shot peening and its effect on corrosion resistance of 1Cr18Ni9Ti stainless steel, Surf. Coat. Technol. 200 (2006) 4777–4781.
[29] K. Lu, J. Lu, Nanostructured surface layer on metallic materials induced by surface mechanical attrition treatment, Mater. Sci. Eng. A 375–377 (2004) 38–45.
[30] T.O. Olugbade, Stress corrosion cracking and precipitation strengthening mechanism in TWIP steels: progress and prospects, Corros. Rev. 38 (2020) 473–488.
[31] K. Lu, J. Lu, Surface Nanocrystallization (SNC) of metallic materials-presentation of the concept behind a new approach, J. Mater. Sci. Technol. 15 (1999) 193–197.
[32] G. Liu, J. Lu, K. Lu, Surface nanocrystallization of 316L stainless steel induced by ultrasonic shot peening, Mater. Sci. Eng. A 286 (2000) 91–95.
[33] S. Kang, J. Jung, M. Kang, W. Woo, Y. Lee, The effects of grain size on yielding, strain hardening, and mechanical twinning in Fe–18Mn–0.6C–1.5Al twinning-induced plasticity steel. Mater. Sci. Eng. A 652 (2016) 212–220.
[34] I. Gutierrez-Urrutia, D. Raabe, Grain size effect on strain hardening in twinning-induced plasticity steels, Scr. Mater. 66 (2012) 992–996.
[35] G. Dini, R. Ueji, Effect of grain size and grain orientation on dislocations structure in tensile strained TWIP steel during initial stages of deformation, Steel Res. Int. 83 (2012) 374–378.
[36] Y.-K. Lee, Microstructural evolution during plastic deformation of twinning-induced plasticity steels, Scr. Mater. 66 (2012) 1002–1006.
[37] J.W. Christian, S. Mahajan, Deformation twinning, Prog. Mater. Sci. 39 (1995) 1–157.
[38] I. Karaman, H. Sehitoglu, Y.I. Chumlyakov, H.J. Maier, I.V. Kireeva, Extrinsic stacking faults and twinning in Hadfield manganese steel single crystals, Scr. Mater. 44 (2001) 337–343.
[39] I. Karaman, H. Sehitoglu, K. Gall, Y.I. Chumlyakov, H.J. Maier, Deformation of single crystal Hadfield steel by twinning and slip, Acta Mater. 48 (2000) 1345–1359.
[40] L. Bracke, L. Kestens, J. Penning, Direct observation of the twinning mechanism in an austenitic Fe–Mn–C steel. Scr. Mater. 61 (2009) 220–222.
[41] H. Idrissi, K. Renard, L. Ryelandt, D. Schryvers, P.J. Jacques, On the mechanism of twin formationin Fe–Mn–C TWIPsteels. ActaMater 58 (2010) 2464–2476.
[42] T.O. Olugbade, B.O. Omiyale, O.T. Ojo, M.K. Adeyeri, Stress-corrosion and corrosion-fatigue properties of surface-treated aluminium alloys for structural applications, Chem. Afr. 6 (2023) 1699–1708.
[43] T. Hu, C.S. Wen, G.Y. Sun, S.L. Wu, C.L. Chu, Z.W. Wu, G.Y. Li, J. Lu, K.W. K. Yeung, P.K. Chu, Wear resistance of NiTi alloy after surface mechanical attrition treatment, Surf. Coat. Technol. 205 (2010) 506–510.
[44] G. Xiang, T. Yang, J. Guo, J. Wang, B. Liu, S. Chen, Optimization transient wear and contact performances of water-lubricated bearings under fluid-solid-thermal coupling condition using profile modification, Wear 502-503 (2022) 204379, https://doi.org/10.1016/j.wear.2022.204379.
[45] Q. Gong, M. Cai, Y. Gong, M. Chen, T. Zhu, Q. Liu, Grinding surface and subsurface stress load of nickel-based single crystal superalloy DD5, Precis. Eng. 88 (2024) 354–366, https://doi.org/10.1016/j.precisioneng.2024.02.017.

[46] T.O. Olugbade, Passive film analysis and corrosion study of steel type 301 after mechanical deformation, MRS Adv. 7 (2022) 886–891.
[47] T.O. Olugbade, B.O. Omiyale, Corrosion study and surface analysis of the passivation film on surface-deformed AISI 304 stainless steel, Chem. Afr. 5 (2022) 1663–1670.
[48] T.O. Olugbade, B.O. Omiyale, Corrosion resistance of surface-conditioned 301 and 304 stainless steels by salt spray test, Analecta Tech. Szeged. 15 (2021) 9–19.
[49] H.Q. Sun, Y.N. Shi, M.-X. Zhang, K. Lu, Surface alloying of an Mg alloy subjected to surface mechanical attrition treatment, Surf. Coat. Technol. 202 (2008) 3947–3953.
[50] Y.Q. Fu, N.L. Loh, J. Wei, B.B. Yan, P. Hing, Friction and wear behaviour of carbon nitride films deposited on plasma nitrided Ti–6Al–4V, Wear 237 (2000) 12.